Rock Mech. Rock Engng. (2003) 36 (3), 237–253
DOI 10.1007/s00603-002-0048-7

Rock Mechanics and Rock Engineering
Printed in Austria

Technical Note

Dimensionless Graphical Representation of the Exact Elasto-plastic Solution of a Circular Tunnel in a Mohr-Coulomb Material Subject to Uniform Far-field Stresses

By

C. Carranza-Torres

Geomechanical Engineering Section, Itasca Consulting Group Inc., Minneapolis, U.S.A.

Received October 8, 2001; accepted December 4, 2002;
Published online February 25, 2003

Keywords: Circular tunnel, elasto-plastic solution, graphical representation, scaling rule.

1. Introduction

A fundamental problem in rock mechanics is that of determining the extent of the plastic zone and radial convergence for a circular tunnel excavated in a Mohr-Coulomb perfectly plastic material subject to uniform far-field stresses. The solution to this problem has applications in the civil, mining and petroleum engineering industries. Examples include the design of tunnel liners according to the Convergence-Confinement method, the stability analysis of underground galleries and shafts in mines, the stability analysis of boreholes for site investigations and for petroleum and gas extraction.

Closed-form analytical solutions for this problem have been presented by many authors in the past. Brown et al. (1983) presented a thorough literature review of analytical solutions published by that time. Many of these solutions include simplifying assumptions, specifically in the derivation of expressions for radial convergence around the tunnel. A few other solutions present a rigorous (correct) treatment for the radial convergence. Among these 'exact' solutions one can mention the ones by Salençon (1969), Detournay (1986), Duncan Fama (1993) and Panet (1995).

This paper presents a graphical representation of the exact solution for this fundamental problem. This graphical representation uses a scaling rule for Mohr-Coulomb elasto-plastic behavior discussed by Anagnostou and Kovari

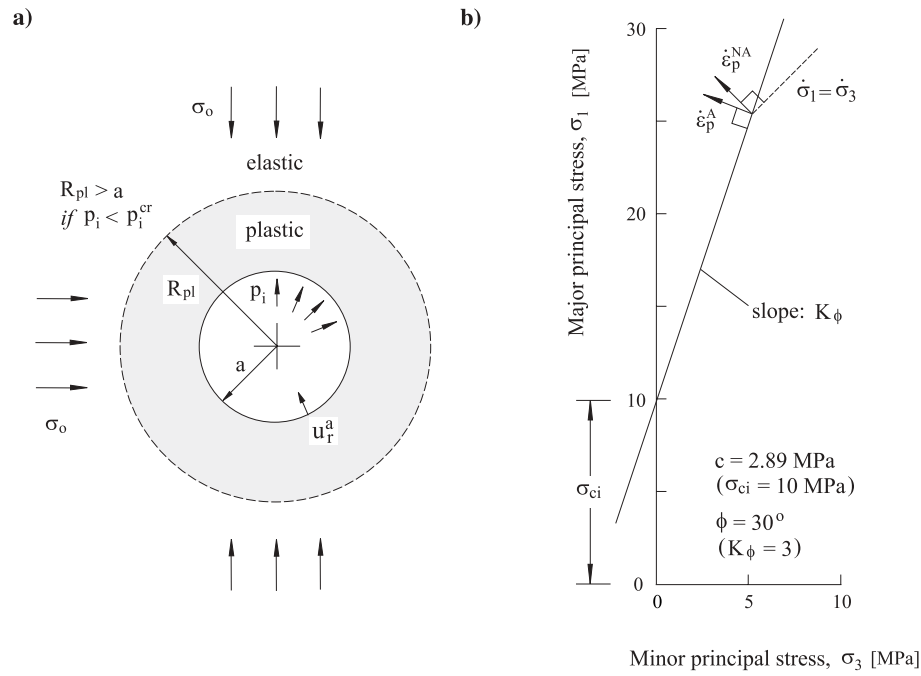

Fig. 1. a) Circular tunnel in a Mohr-Coulomb elasto-plastic material subject to uniform far-field stresses and internal pressure. **b)** Mohr-Coulomb failure envelope in terms of principal stresses

(1993). It should be noted that a similar graphical representation has been discussed by Kovari (1985) and Kovari (1986), although in that case the author introduced simplifications in the formulation for radial convergence around the tunnel.

The graphical representation described in this paper applies to both frictional-cohesive and cohesive-only Mohr-Coulomb materials. The representation can also be applied in the construction of 'Universal' Ground Reaction curves. These diagrams summarize every possible relationship between internal pressure and wall convergence obtainable from the fundamental (rigorous) solution of symmetrical excavation of a circular tunnel in a Mohr-Coulomb material.

2. Description of the Problem

The problem considered in this paper is represented in Fig. 1a. A long circular tunnel of radius a that is subject to far-field stresses σ_o and internal pressure p_i is excavated in a perfectly-plastic Mohr-Coulomb material (plane strain conditions are considered). As a result of decreasing the internal pressure p_i below the initial value σ_o, the wall of the tunnel converges a certain amount u_r^a. When the internal pressure p_i falls below a critical value p_i^{cr} a circular failure zone of radius R_{pl} develops (concentrically) around the tunnel.

The elastic behavior of the material is characterized by the Shear Modulus G

and the Poisson's ratio ν – the Young's Modulus E is related to the Shear Modulus G according to the classical relationship $E = 2G(1 + \nu)$.

The plastic behavior of the material is characterized by the internal friction angle ϕ, the cohesion c, and the dilation angle ψ.

According to the Mohr-Coulomb failure criterion, the relationship between major and minor principal stresses, σ_1 and σ_3 respectively, is given by the following relationship

$$\sigma_1 = K_\phi \sigma_3 + \sigma_{ci}, \tag{1}$$

where K_ϕ is the *passive reaction* coefficient, that is computed from the internal friction angle ϕ as follows,

$$K_\phi = \frac{1 + \sin\phi}{1 - \sin\phi} \tag{2}$$

and σ_{ci} is the unconfined compression strength that is computed from the cohesion c and the coefficient K_ϕ according to,

$$\sigma_{ci} = 2c\sqrt{K_\phi}. \tag{3}$$

The Mohr-Coulomb failure criterion (Eq. (1)) is represented in Fig. 1b. The coefficient K_ϕ is the slope of the linear failure envelope and the unconfined compression strength σ_{ci} is the intercept of the linear envelope and the vertical axis.

The volumetric response of the material is controlled by the dilation angle ψ. If the dilation angle is zero (i.e., $\psi = 0^\circ$) then the plastic flow rule is said to be *non-associated* and there is no volumetric change while the material plastifies. If the dilation angle is equal to the internal friction angle ($\psi = \phi$), then the plastic flow rule is said to be *associated* and the material undergoes volumetric expansion while it plastifies.

The dilation angle ψ enters the elasto-plastic formulation presented in this paper through the parameter K_ψ, that has a similar form as the parameter K_ϕ, i.e.,

$$K_\psi = \frac{1 + \sin\psi}{1 - \sin\psi}. \tag{4}$$

The parameter K_ψ controls the inclination of the plastic-strain rate vector represented in Fig. 1b. If the plastic flow-rule is non-associated with $K_\psi = 1$ (or zero friction angle), then the vector $\dot{\varepsilon}_p^{\mathrm{NA}}$ is normal to the line $\dot{\sigma}_1 = \dot{\sigma}_3$. If the flow-rule is associated with $K_\psi = K_\phi$ then the vector $\dot{\varepsilon}_p^{\mathrm{A}}$ is normal to the yield envelope given by Eq. (1).

3. Solution for the Case of Frictional-cohesive Material ($\phi > 0^\circ$ and $c \neq 0$)

Anagnostou and Kovari (1993) showed that the cohesion c (or alternatively the unconfined compression strength σ_{ci}) can be 'hidden' in the Mohr-Coulomb failure criterion (1) if the principal stresses σ_1 and σ_3 are transformed as follows

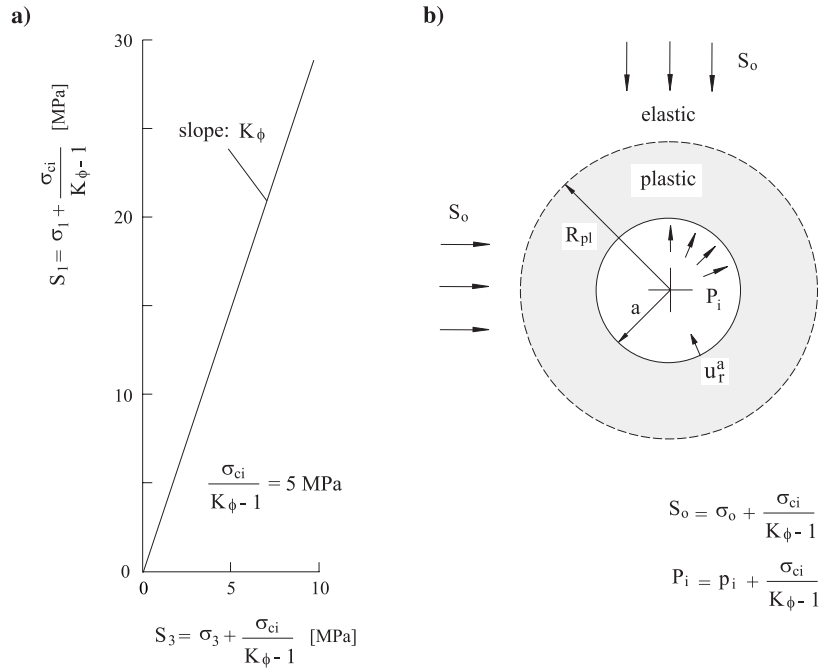

Fig. 2. a) Mohr-Coulomb failure envelope in terms of transformed principal stresses. **b)** Problem of tunnel excavation in the 'transformed' Mohr-Coulomb elasto-plastic material

$$S_1 = \sigma_1 + \frac{\sigma_{ci}}{K_\phi - 1} \tag{5}$$

$$S_3 = \sigma_3 + \frac{\sigma_{ci}}{K_\phi - 1}. \tag{6}$$

Note that according to Eqs. (2) and (3) the term $\sigma_{ci}/(K_\phi - 1)$ in the equations above is equal to the term $c/\tan\phi$.

With the principal stresses transformed as in Eqs. (5) and (6), the Mohr-Coulomb failure criterion (1) is written in the simpler form

$$S_1 = K_\phi S_3. \tag{7}$$

Figure 2a represents the same failure envelope in Fig. 1b, but this time in terms of transformed stresses S_1 and S_3. The new failure envelope passes through the origin of the reference system so the material can be regarded as cohesionless or purely frictional.

The formulation of the problem introduced in Fig. 1a can be conveniently simplified if the stress variables entering the problem are transformed, as in Eqs. (5) and (6).

Figure 2b represents the same problem in Fig. 1a, but in terms of transformed variables S_o, P_i and P_i^{cr} that are computed from the variables σ_o, p_i and p_i^{cr} respectively, as in Eqs. (5) and (6), i.e.,

$$S_o = \sigma_o + \frac{\sigma_{ci}}{K_\phi - 1}, \tag{8}$$

$$P_i = p_i + \frac{\sigma_{ci}}{K_\phi - 1}, \tag{9}$$

$$P_i^{cr} = p_i^{cr} + \frac{\sigma_{ci}}{K_\phi - 1}. \tag{10}$$

A rigorous solution for the transformed problem in Fig. 2b is discussed in Carranza-Torres (2002). The solution will be presented here without a demonstration (the interested reader is referred to the article mentioned above). It should be noted nevertheless that the following expressions are completely equivalent to the other rigorous solutions listed in the Introduction to this paper.

The transformed critical internal pressure P_i^{cr}, below which the plastic zone develops, depends on the value of transformed far-field stress S_o and the parameter K_ϕ as follows

$$\frac{P_i^{cr}}{S_o} = \frac{2}{K_\phi + 1}. \tag{11}$$

If the given value of transformed internal pressure P_i is below the critical value P_i^{cr} (i.e., $P_i < P_i^{cr}$), then the radius R_{pl} of the plastic zone is

$$\frac{R_{pl}}{a} = \left[\frac{P_i^{cr}}{P_i}\right]^{1/(K_\phi - 1)}. \tag{12}$$

For this case the radial convergence at the tunnel wall is

$$\frac{u_r^a}{a}\frac{2G}{S_o - P_i^{cr}} = \frac{(K_\psi - 1)(K_\phi - 1) - 2C}{(K_\psi + 1)(K_\phi - 1)} + \frac{2(K_\phi + K_\psi) + 2C}{(K_\psi + 1)(K_\phi + K_\psi)}\left(\frac{R_{pl}}{a}\right)^{K_\psi + 1} + \frac{2C}{(K_\phi + K_\psi)(K_\phi - 1)}\left(\frac{a}{R_{pl}}\right)^{K_\phi - 1}, \tag{13}$$

where the constant C is

$$C = (1 - \nu)(K_\phi K_\psi + 1) - \nu(K_\phi + K_\psi). \tag{14}$$

If the given value of transformed internal pressure P_i is above the critical value P_i^{cr} (i.e., $P_i > P_i^{cr}$), then the wall convergence is given by Lamé's classical solution (see for example Jaeger and Cook, 1979),

$$\frac{u_r^a}{a}\frac{2G}{S_o} = 1 - \frac{P_i}{S_o}. \tag{15}$$

Equations (11), (12) and (13) are represented in Figs. 3 and 4 – Fig. 4a considers the case of non-associated flow rule with dilation angle $\psi = 0°$ while Fig. 4b considers the case of associated flow rule with dilation angle $\psi = \phi$.

To illustrate the application of these diagrams we consider the problem of excavating a deep gallery in hard rock, as represented in Fig. 5a (geometry

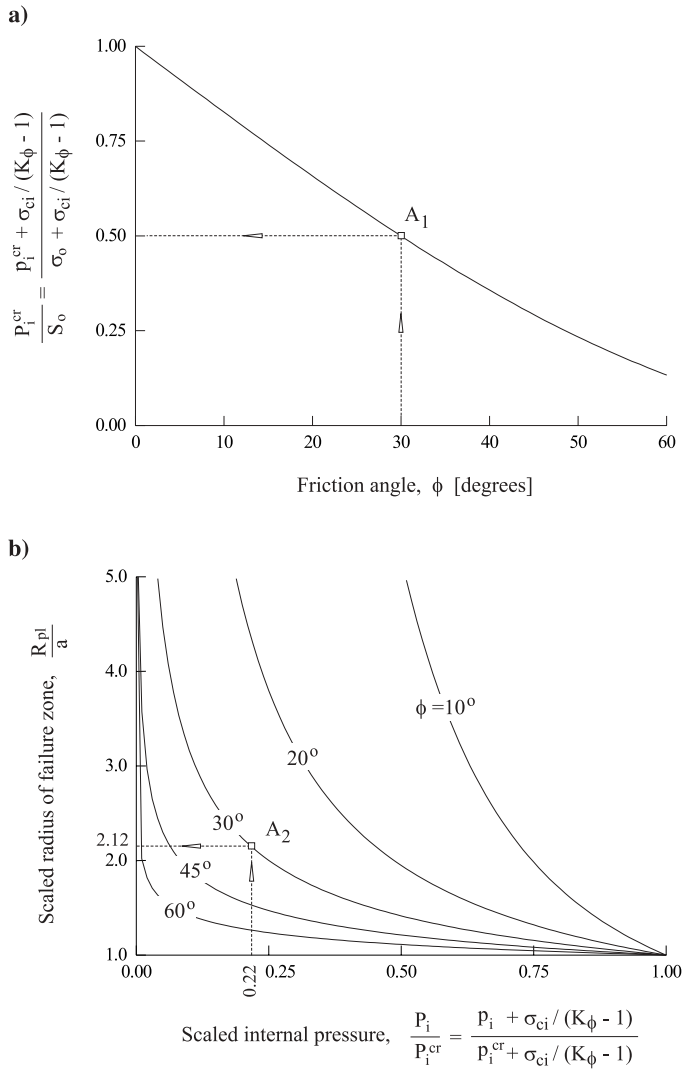

Fig. 3. Charts for the determination of **a)** critical internal pressure below which the failure zone develops around the tunnel and **b)** radius of the failure zone in the case of frictional-cohesive material ($\phi > 0^\circ$ and $c \neq 0$)

dimensions, loading conditions and elasto-plastic properties are listed under the heading *Data* in the figure). The objective is to compute the critical internal pressure below which the plastic zone starts to develop, the extent of the plastic zone, and the convergence of the tunnel wall.

The first step of the solution is to compute the transformed loading conditions according to Eqs. (8) through (10) – see *Step 1* in Fig. 5. The second step is to compute the critical value of internal pressure from Fig. 3a – see *Step 2* in Fig. 5. For this particular problem $P_i^{cr}/S_o = 0.5$ (see point A_1 in Fig. 3a) and since

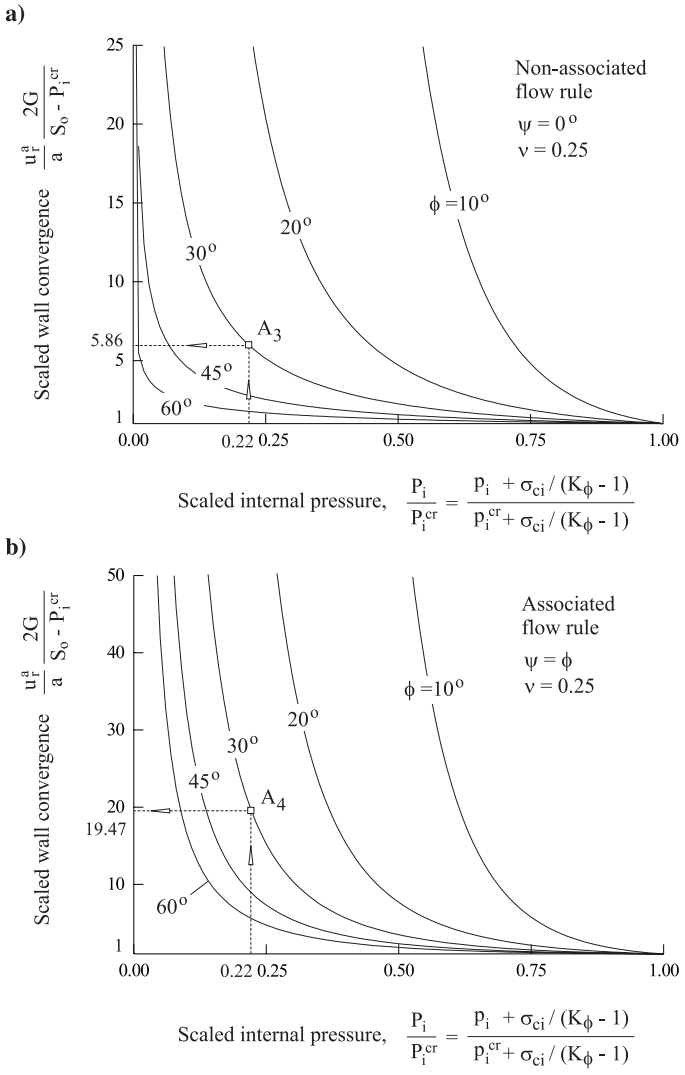

Fig. 4. Charts for the determination of the wall radial displacement for **a)** associated and **b)** non-associated flow rules for the case of frictional-cohesive material ($\phi > 0°$ and $c \neq 0$)

$P_i/S_o = 0.11$ then $P_i < P_i^{cr}$ and the plastic zone actually develops. The third step is to compute the value of radius of plastic zone from Fig. 3b – see *Step 3* in Fig. 5. For this particular problem the extent of the plastic zone is 2.12 times the radius of the tunnel – see point A_2 in Fig. 3b. The fourth step is to compute the value of wall convergence from Fig. 4a and 4b – see *Step 4* in Fig. 5. In this case the scaled values of radial convergence are $(u_r^a/a)(2G/(S_o - P_i^{cr})) = 5.86$ and $(u_r^a/a)(2G/(S_o - P_i^{cr})) = 19.47$ for non-associated and associated flow rule respectively (see points A_3 and A_4 in Fig. 4), so the final convergence are 7% and 22% times the radius of the tunnel (respectively).

DATA

$a = 2$ m

$\sigma_o = 40$ MPa
$p_i = 0$ MPa

$\sigma_{ci} = 10$ MPa

$\phi = 30^o$

i) $\psi = 0^o$
ii) $\psi = 30^o$

$G = 1$ GPa
$\nu = 0.25$

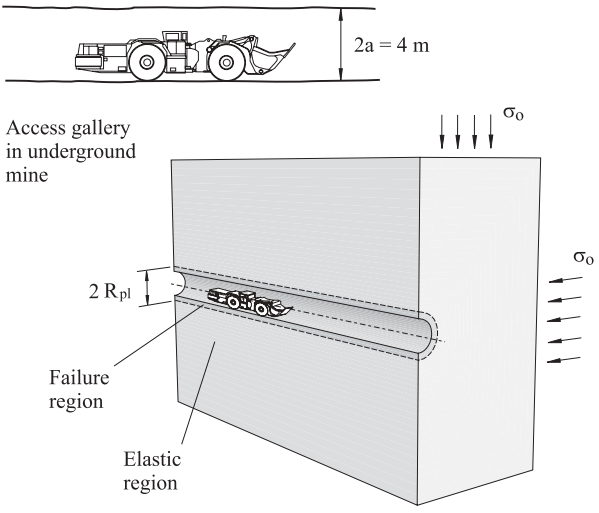

STEP 1: Intermediate computations

$$K_\phi = 3.0, \quad \frac{\sigma_{ci}}{K_\phi - 1} = 5 \text{ MPa} \quad \Rightarrow \quad S_o = \sigma_o + \sigma_{ci} / (K_\phi - 1) = 45 \text{ MPa}$$

$$P_i = p_i + \sigma_{ci} / (K_\phi - 1) = 5 \text{ MPa}$$

STEP 2: Critical internal pressure at the elastic limit

From Figure 3a, for $\phi = 30^o$ $\Rightarrow$ $\dfrac{P_i^{cr}}{S_o} = 0.5$ $\therefore$ $P_i^{cr} = 22.5$ MPa

and $p_i^{cr} = 17.5$ MPa

STEP 3: Radius of the plastic zone

From Figure 3b, for $\phi = 30^o$ and $\dfrac{P_i}{P_i^{cr}} = 0.22$ $\Rightarrow$ $\dfrac{R_{pl}}{a} = 2.12$

STEP 4: Wall convergence

a) Non-associated flow rule, $\psi = 0^o$

From Figure 4a, for $\phi = 30^o$ and $\dfrac{P_i}{P_i^{cr}} = 0.22$ $\Rightarrow$ $\dfrac{u_r^a}{a} \dfrac{2G}{S_o - P_i^{cr}} = 5.86$

$\therefore$ $\dfrac{u_r^a}{a} = 7\%$

b) Associated flow rule, $\psi = \phi$

From Figure 4b, for $\phi = 30^o$ and $\dfrac{P_i}{P_i^{cr}} = 0.22$ $\Rightarrow$ $\dfrac{u_r^a}{a} \dfrac{2G}{S_o - P_i^{cr}} = 19.47$

$\therefore$ $\dfrac{u_r^a}{a} = 22\%$

Fig. 5. Example of elasto-plastic analysis of a gallery in a mine showing the application of Figs. 3 and 4 (gravity is neglected in the problem and conditions of plane strain are considered for sections perpendicular to the axis of the gallery)

4. Solution for the Case of Frictionless Purely-cohesive Material ($\phi = 0^\circ$ and $c \neq 0$)

The transformation discussed by Anagnostou and Kovari (1993) does not apply in the case of frictionless material, since the term $K_\phi - 1$ in Eqs. (8) through (10) becomes zero and the transformed stresses become indeterminate.

The solution for the problem in Fig. 1a can still be found from the solution presented above (Eqs. (11) through (15)) if the values of transformed stresses S_o, P_i and P_i^{cr} are replaced by their definition in Eqs. (8), (9) and (10) and the limit $K_\phi \to 1$ is computed in the resulting expressions using L'Hospital rule.

For the frictionless Mohr-Coulomb material (also known as the Tresca material), the solution is given by the following expressions.

The critical internal pressure p_i^{cr} is

$$\frac{p_i^{cr}}{\sigma_o} = 1 - \frac{1}{2}\frac{\sigma_{ci}}{\sigma_o}. \tag{16}$$

For the case $p_i < p_i^{cr}$ the extent of the failure zone is

$$\frac{R_{pl}}{a} = \exp\left[\left(1 - \frac{p_i}{p_i^{cr}}\right)\left(\frac{\sigma_o}{\sigma_{ci}} - \frac{1}{2}\right)\right], \tag{17}$$

and the corresponding radial convergence is

$$\frac{u_r^a}{a}\frac{2G}{\sigma_o - p_i^{cr}} = \frac{K_\psi - 1 - 2(1-2\nu)}{K_\psi + 1} + \frac{4(1-\nu)}{K_\psi + 1}\left(\frac{R_{pl}}{a}\right)^{K_\psi + 1} + 2(1-2\nu)\ln\left(\frac{a}{R_{pl}}\right). \tag{18}$$

For the case $p_i > p_i^{cr}$ the wall radial convergence is obtained again from Lamé's solution, i.e.,

$$\frac{u_r^a}{a}\frac{2G}{\sigma_o} = 1 - \frac{p_i}{\sigma_o}. \tag{19}$$

Equations (16), (17) and (18) are represented graphically in Figs. 6 and 7. An example showing the application of these diagrams is presented in Fig. 8. The example considers the analysis of a section of borehole drilled in a non-frictional material (e.g., in clay) and with internal support provided by a material of lower density (e.g., by bentonite). As a simplification, gravity is neglected and conditions of plane strain are considered for sections perpendicular to the borehole axis (the value of σ_o considered in Fig. 8 corresponds then to the mean value of horizontal stress at the depth of interest). Results for this problem are presented in Fig. 8.

5. 'Universal' form of the Ground Reaction Curve in Mohr-Coulomb Perfectly-plastic Materials

As mentioned in the Introduction to this paper, the Ground Reaction curve is the graphical representation of the relationship between decreasing internal pressure

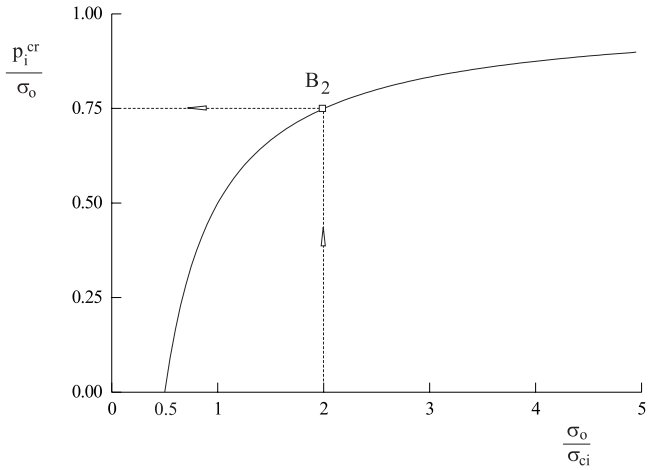

Fig. 6. Chart for the determination of the critical internal pressure below which the failure zone develops around the tunnel for the case of frictionless purely-cohesive material ($\phi = 0°$ and $c \neq 0$)

p_i and resulting wall convergence u_r^a (see Fig. 1a). The ground reaction curve is the basis of tunnel support design according to the Convergence-Confinement method (see for example, Hoek and Brown, 1980; Brady and Brown, 1993; Hoek et al., 1995).

A 'Universal' form of the ground reaction curve for circular tunnels in Mohr-Coulomb perfectly-plastic material can be constructed from the expressions presented earlier.

For example, in the case of frictional-cohesive material ($\phi > 0°$; $c \neq 0$), replacing Eqs. (11) and (12) into Eq. (13), the plastic part of the ground reaction curve is given by

$$\frac{u_r^a}{a}\frac{2G}{S_o} = \frac{K_\phi - 1}{K_\phi + 1}\left[\frac{(K_\psi - 1)(K_\phi - 1) - 2C}{(K_\psi + 1)(K_\phi - 1)} + \frac{2(K_\phi + K_\psi) + 2C}{(K_\psi + 1)(K_\phi + K_\psi)}\left(\frac{K_\phi + 1}{2}\frac{P_i}{S_o}\right)^{-(K_\psi+1)/(K_\phi-1)} + \frac{2C}{(K_\phi + K_\psi)(K_\phi - 1)}\frac{K_\phi + 1}{2}\frac{P_i}{S_o}\right]. \tag{20}$$

Similarly, for the case of frictionless purely-cohesive material ($\phi = 0°$; $c \neq 0$), replacing Eqs. (16) and (17) into Eq. (18),

$$\frac{u_r^a}{a}\frac{2G}{\sigma_o} = \frac{1}{2}\frac{\sigma_{ci}}{\sigma_o}\left[\frac{K_\psi - 1 - 2(1-2\nu)}{K_\psi + 1} + \frac{4(1-\nu)}{K_\psi + 1}\exp\left[(K_\psi + 1)\left(\frac{\sigma_o}{\sigma_{ci}} - \frac{p_i}{\sigma_o}\frac{\sigma_o}{\sigma_{ci}} - \frac{1}{2}\right)\right] - 2(1-2\nu)\left(\frac{\sigma_o}{\sigma_{ci}} - \frac{p_i}{\sigma_o}\frac{\sigma_o}{\sigma_{ci}} - \frac{1}{2}\right)\right]. \tag{21}$$

The 'Universal' Ground Reaction curves defined by Eqs. (20) and (21) are

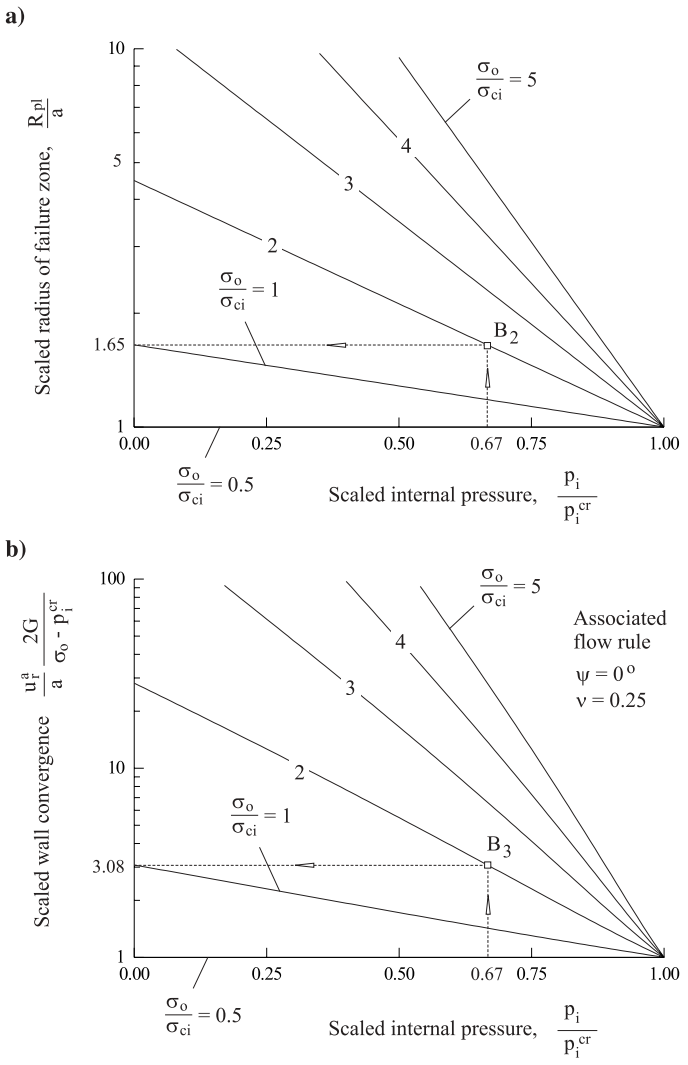

Fig. 7. Charts for the determination of **a)** the radius of the failure zone and **b)** the wall radial convergence for the case of frictionless purely-cohesive material ($\phi = 0^\circ$ and $c \neq 0$)

represented graphically in Figs. 9 and 10 respectively. Note that Fig. 9a corresponds to non-associated flow rule ($\psi = 0^\circ$), while 9b corresponds to associated flow rule ($\psi = \phi$). The linear curve in these diagrams represents the elastic behavior of the tunnel – note that the scaling of the horizontal axis is such that the scaled convergence is equal to 1 if the tunnel in Fig. 2b is unsupported; i.e., $P_i/S_o = 0$. The non-linear curves in these diagrams correspond to the plastic behavior of the tunnel – the different curves are for different values of internal friction angle ϕ.

In essence, every Ground Reaction curve that can be constructed with the rigorous solution of the circular tunnel problem in a Mohr-Coulomb material will

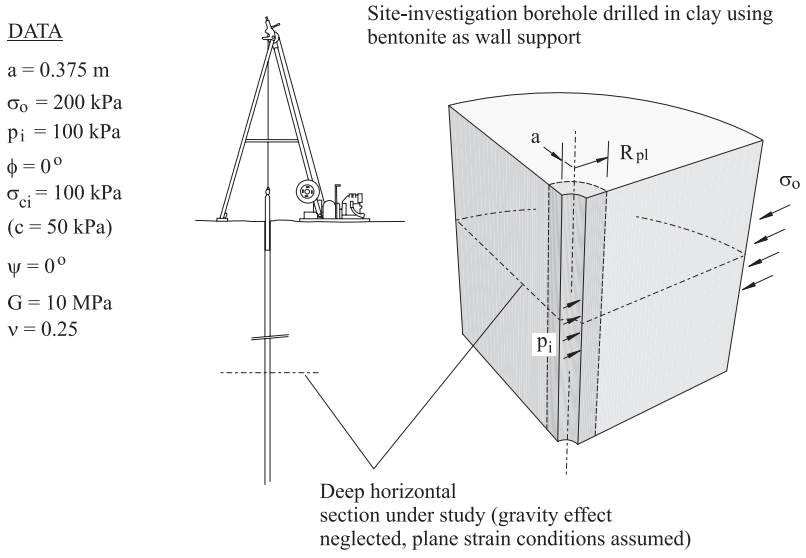

STEP 1: Critical internal pressure at the elastic limit

From Figure 6, for $\frac{\sigma_o}{\sigma_{ci}} = 2 \Rightarrow \frac{p_i^{cr}}{\sigma_o} = 0.75 \therefore p_i^{cr} = 150$ kPa

STEP 2: Radius of the plastic zone

From Figure 7a, for $\frac{p_i}{p_i^{cr}} = 0.67$ and $\frac{\sigma_o}{\sigma_{ci}} = 2 \Rightarrow \frac{R_{pl}}{a} = 1.65$

STEP 3: Wall convergence (for no-plastic dilation case)

From Figure 7b, for $\frac{p_i}{p_i^{cr}} = 0.67$ and $\frac{\sigma_o}{\sigma_{ci}} = 2$

$$\Rightarrow \frac{u_r^a}{a} \frac{2G}{\sigma_o - p_i^{cr}} = 3.08 \quad \therefore \frac{u_r^a}{a} = 0.77\%$$

Fig. 8. Example of elasto-plastic analysis of a vertical borehole in clay showing the application of Figs. 6 and 7 (gravity is neglected in the problem and conditions of plane strain are considered for sections perpendicular to the axis of the borehole)

be contained in these curves. For example, the points indicated as C and D in Figs. 9 and 10 respectively represent the solution for the examples discussed in Figs. 5 and 8.

A potential practical application of these diagrams is the interpretation of results from parametric studies of tunnel convergence. Studies of this type in which elasto-plastic models like the one in Fig. 1a are 'fed' with Mohr-Coulomb parameters estimated from the quality of the rock mass have been presented, for example, by Hoek (2001) – relationships between Mohr-Coulomb parameters and the quality of the rock mass for applications in tunnel design can be found in Hoek et al. (2002). To illustrate the application of the diagrams, let us consider

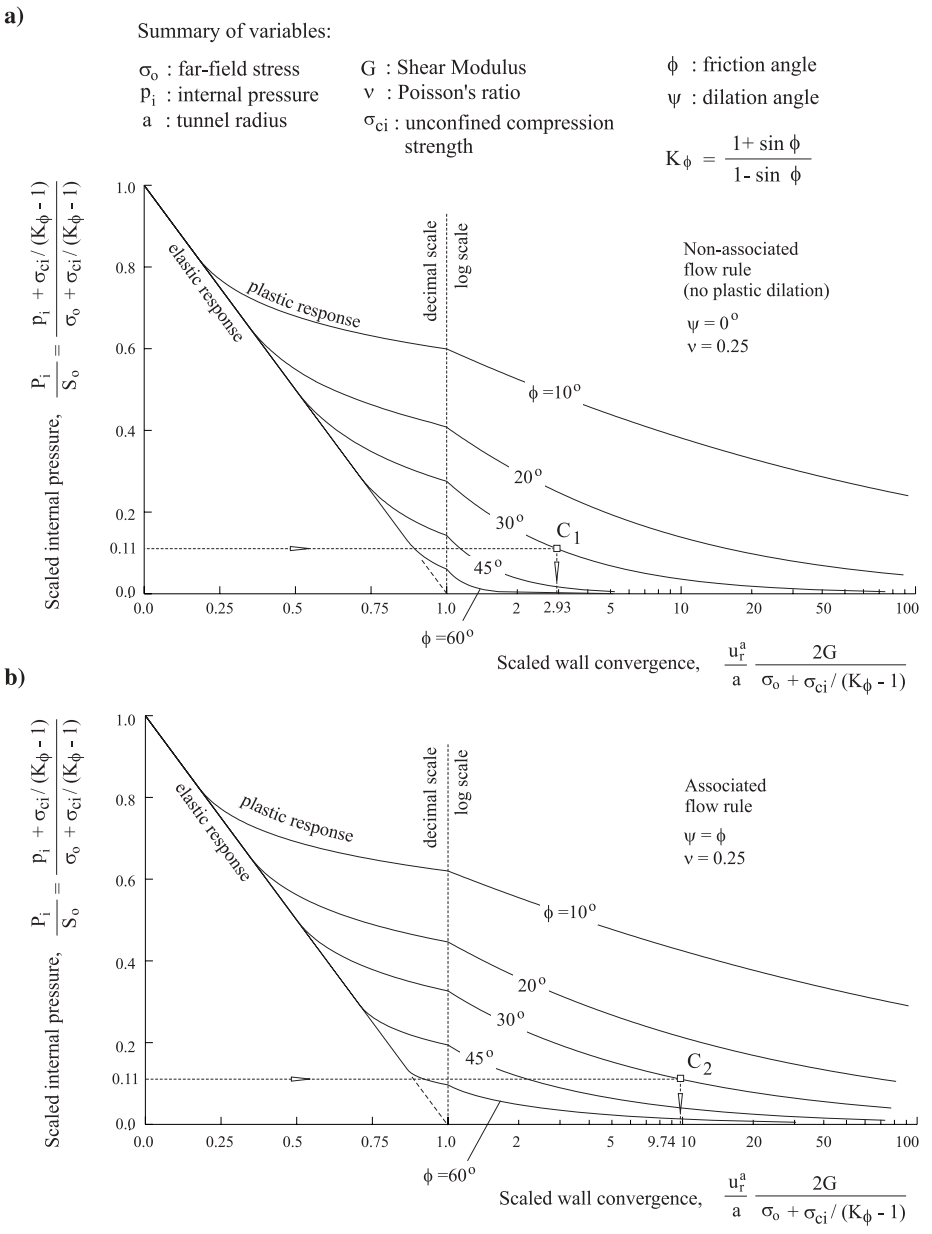

Fig. 9. 'Universal' Ground Reaction curves for a tunnel excavated in frictional-cohesive elasto-plastic Mohr-Coulomb material for **a)** non-associated ($\psi = 0°$) and **b)** associated ($\psi = \phi$) flow rules

the results obtained from statistical analysis of tunnel cases in which the friction angle of the material was kept constant (e.g., $\phi = 30°$) and the 'exact' solution of the tunnel problem (as given by Eqs. (8) through (15) or by the solutions mentioned in the Introduction to this paper) was applied to find the relationship

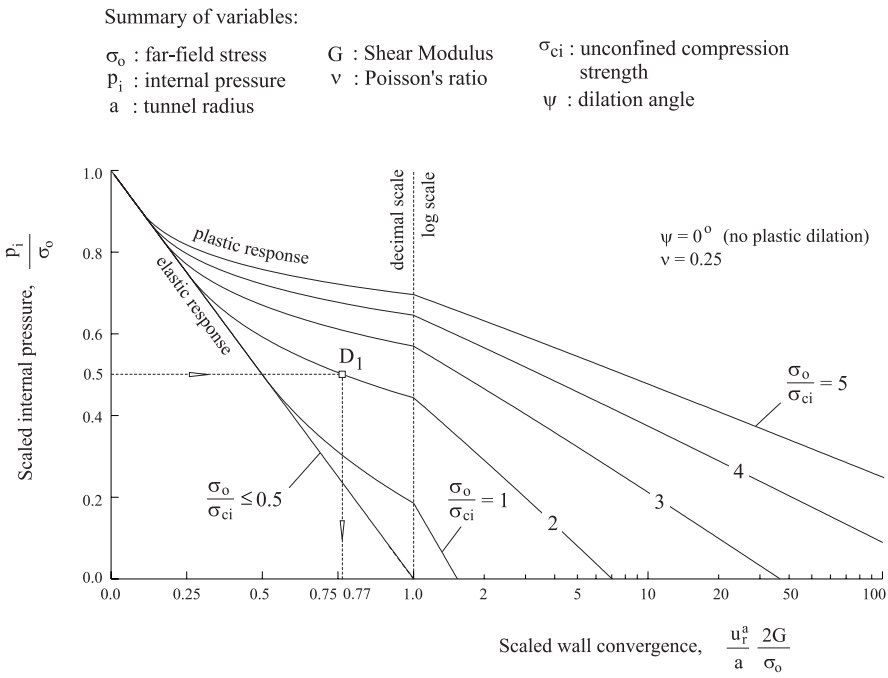

Fig. 10. 'Universal' Ground Reaction curve for a tunnel excavated in frictionless, purely-cohesive, elasto-plastic material

between internal pressure and wall convergence for different values of far-field stresses σ_o, internal pressure p_i, unconfined compression strength σ_{ci}, Shear Modulus G and tunnel radius a (see Fig. 11a).

The different points in Fig. 11b represent results of scaled internal pressure p_i/σ_o and scaled wall convergence u_r^a/a for randomly generated cases with properties in the ranges indicated in Fig. 11a.

Figure 11c represents the same results as in Fig. 11b, but this time plotted on the 'Universal' Ground Reaction curve of Fig. 9a. The random nature of the results has clearly disappeared and all points align now to the fundamental Ground Reaction curve for the value of friction angle used in the generation of cases (i.e., the value $\phi = 30°$).

6. Discussion

The dimensionless graphical solution presented in this paper can be conveniently used to perform a rigorous elasto-plastic analysis of circular tunnel excavation problems in perfectly Mohr-Coulomb material under hydrostatic loading, for both frictional-cohesive materials and frictionless purely-cohesive materials.

The scaling rule considered by Anagnostou and Kovari (1993) can be easily applied to the solution of elasto-plastic problems involving the Mohr-Coulomb failure criterion. A practical application of this particular form of scaling was

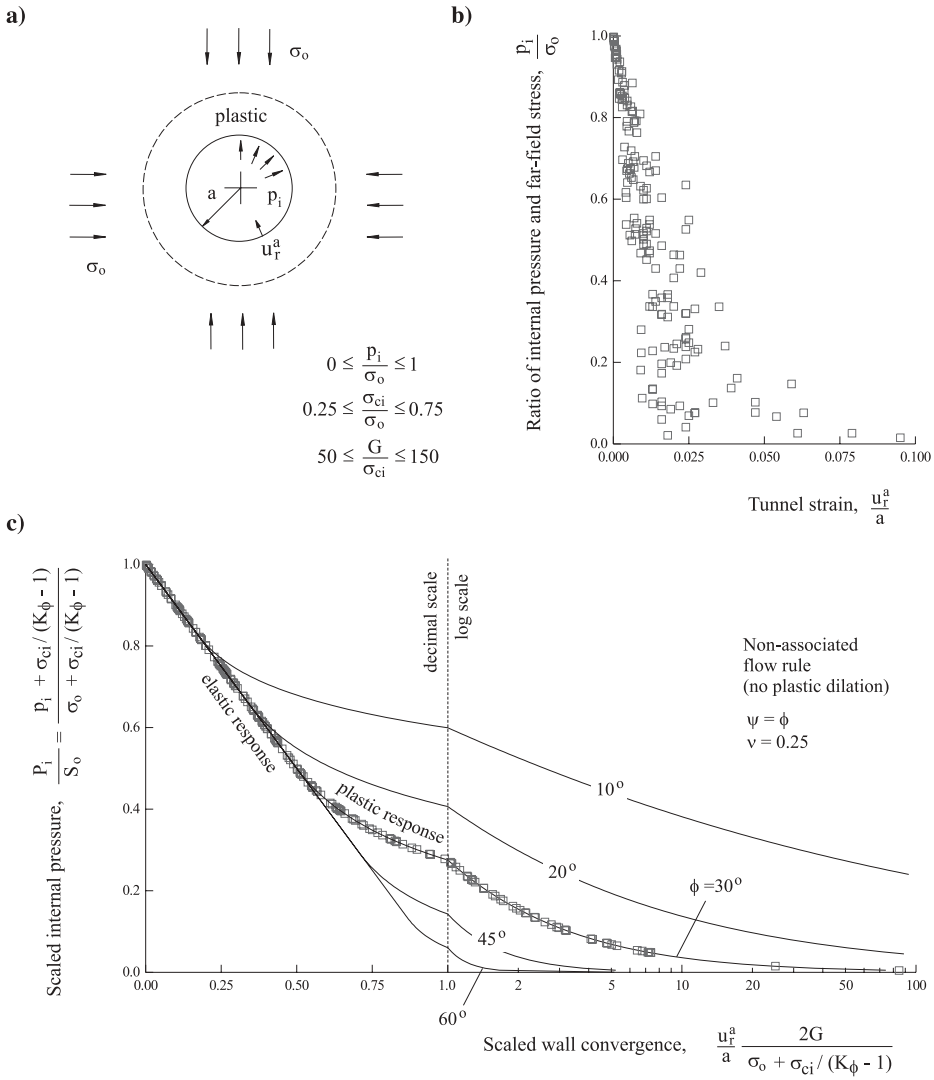

Fig. 11. a) Randomly generated tunnel cases. **b)** Representation of the results in the *classical* Ground Reaction curve. **c)** Representation of the results in the 'Universal' Ground Reaction curve

illustrated here with the construction of 'Universal' Ground Reaction curves for tunnels in a Mohr-Coulomb perfectly plastic material.

The same scaling rule can be applied, under certain conditions, to the case of perfectly brittle Mohr-Coulomb failure criterion. Carranza-Torres et al. (2002) describes how the 'Universal' Ground Reaction curve for this material behavior can be obtained.

The advantages that the transformation rule brings in the representation of results of tunnel problems in Mohr-Coulomb materials (mainly in terms of simplification of the representation), make it worth examining the possibility of

deriving diagrams similar to the ones presented here for other fundamental solutions, such as the solution of a circular tunnel subject to non-hydrostatic loading derived by Detournay and Fairhurst (1987) and Detournay and St. John (1988).

References

Anagnostou, G., Kovari, K. (1993): Significant parameters in elastoplastic analysis of underground openings. ASCE J. Geotech. Eng. Div. 119(3), 401–419.

Brady, B. G. H., Brown, E. T. (1993): Rock Mechanics for Underground Mining (2nd edn.). Chapman & Hall, London

Brown, E. T., Bray, J. W., Ladanyi, B., Hoek, E. (1983): Ground response curves for rock tunnels. ASCE J. Geotech. Eng. Div. 109(1), 15–39.

Carranza-Torres, C. (2002): Dimensionless charts for the evaluation of the elasto-plastic response of tunnels in rock. In: Bawden, H. R. W., Curran, J., Telesnicki, M. (Eds.), Proceedings of NARMS-TAC 2002. Mining Innovation and Technology, Toronto, 10 July 2002, University of Toronto, pp. 1133–1143.

Carranza-Torres, C., Alonso, E., Alejano, L. R., Varas, F., Fdez-Manin, G. (2002): Elasto-plastic analysis of deep tunnels in brittle rock using a scaled form of the Mohr-Coulomb failure criterion. In: Bawden, H. R. W., Curran, J., Telesnicki, M. (Eds.), Proceedings of NARMS-TAC 2002. Mining Innovation and Technology, Toronto, 10 July 2002, University of Toronto, pp. 283–293.

Detournay, E. (1986): Elastoplastic model of a deep tunnel for a rock with variable dilatancy. Rock Mech. Rock Engng. 19, 99–108.

Detournay, E., Fairhurst, C. (1987): Two-dimensional elasto-plastic analysis of a long, cylindrical cavity under non-hydrostatic loading. Int. J. Rock Mech. Min. Sci. Geomech. Abstr. 24(4), 197–211.

Detournay, E., St. John, C. (1988): Design charts for a deep circular tunnel under non-uniform loading. Rock Mech. Rock Engng. 21, 119–137.

Duncan Fama, M. E. (1993): Numerical modelling of yield zones in weak rocks. In: Hudson, J. A., Brown, E. T., Fairhurst, C., Hoek, E. (Eds.), Comprehensive rock engineering. Vol. 2. Analysis and design methods. Pergamon Press, Oxford, pp. 49–75.

Hoek, E. (2001): Big tunnels in bad rock. J. Geotechn. and Geoenv. Engng. 127(9), 726–740. The Thirty-Six Karl Terzaghi Lecture.

Hoek, E., Brown, E. T. (1980): Underground excavations in rock. The Institute of Mining and Metallurgy, London.

Hoek, E., Kaiser, P. K., Bawden, W. F. (1995): Support of underground excavations in hard rock. Balkema, Rotterdam.

Hoek, E., Carranza-Torres, C., Corkum, B. (2002): Hoek-Brown failure criterion – 2002 edition. In: H. R. W. Bawden, Curran, J., Telesnicki, M. (Eds.), Proceedings of NARMS-TAC 2002. Mining Innovation and Technology, Toronto, 10 July 2002, University of Toronto, pp. 267–273.

Jaeger, J. C., Cook, N. G. W. (1979): Fundamentals of rock mechanics. John Wiley & Sons, New York.

Kovari, K. (1985): Rock deformation problems when using full-facing cutting equipment in rock. Tunnel 3, 236–244 (Part I), 289–298 (Part II).

Kovari, K. (1986): The determination of the characteristic line from straight line nomogramms. In Proceedings 5th Int. Conf. on Num. Meth. in Geomechanics. Nagoya, Balkema, Rotterdam, pp. 1741–1746.

Panet, M. (1995): Calcul des tunnels par la méthode de convergence-confinement. Press de l'école Nationale des Ponts et Chaussées.

Salençon, J. (1969): Contraction quasi-statique d'une cavité á symétrie sphérique ou cylindrique dans un milieu élastoplastique. Annls Ponts Chauss. 4, 231–236.

Author's address: Dr. Carlos Carranza-Torres, Itasca Consulting Group Inc., 111 Third Av. South, Suite 450, Minneapolis, MN 55 401, U.S.A.; e-mail: cct@itascacg.com